Shear-Enhanced Crystallization in Isotactic Polypropylene. 3. Evidence for a Kinetic Pathway to Nucleation

Guruswamy Kumaraswamy,[†,‡] **Julia A. Kornfield,***[,‡] **Fengji Yeh,**[§] **and Benjamin S. Hsiao**[§]

Division of Chemistry and Chemical Engineering, California Institute of Technology, Pasadena, California 91125.Chemistry Department, State University of New York, Stony Brook, Stony Brook, New York 11794

Received August 7, 2001; Revised Manuscript Received November 5, 2001

ABSTRACT: In situ rheo-optical techniques are combined with synchrotron wide-angle X-ray diffraction (WAXD) to investigate the oriented crystallization precursors that develop upon strongly shearing an isothermal melt of polydisperse isotactic polypropylene (iPP). The "short-term shearing" experimental protocol, developed by Janeschitz-Kriegl and co-workers, is used under conditions previously determined to induce oriented crystallite growth. Surprisingly, the time for these precursors to appear *decreases* with increasing temperature, tracking the melt dynamics of the polymer molecules—a behavior unanticipated by current models. Thus, nucleation proceeds via a "nonclassical" kinetic pathway that effectively eliminates the activation barrier for nucleation. To characterize the importance of chain length distribution for the formation of nucleation precursors, experiments were performed with model bidisperse systems containing a small percentage of high molecular weight iPP blended with lower molecular weight iPP of matched stereoregularity. Oriented crystallization was not observed for the individual components of the blend under the most extreme experimental conditions investigated, but it was readily observed for the bidisperse blend. This suggests that, under intense shear, nucleation of oriented crystallites is governed by the rheologically determined formation of a critical anisotropic configuration of polymer chains in the melt.

1. Introduction

Semicrystalline polymers represent a model system enabling systematic study of the effects of applied fields on first-order phase transitions such as crystallization. In these systems, phase transitions unfold on experimentally accessible time scales and readily accessible deformation rates can perturb the configuration of the slow relaxing macromolecules. Furthermore, an imposed macroscopic stress can be interpreted on a molecular level, directly related to the orientation distribution of the polymer chains.[1] Semicrystalline polymers are technologically important as they comprise about two-thirds of the global polymer production and find wide ranging uses from packaging to such demanding applications as automotive components and biomedical implants. This versatility results primarily from being able to engineer their material properties over orders of magnitude using processing to control the degree of crystallinity and the orientation distribution of crystallites.[2] Virtually all semicrystalline polymers are subjected to intense flow fields as they are processed from the melt state and suitable properties are obtained in the final product by employing empirical rules to select an appropriate combination of resin characteristics and processing conditions.

Despite decades of research, the fundamental nature of the earliest events in crystallization remains mysterious, particularly under the influence of flow. While it is accepted that understanding the factors that influence nucleation are crucial to develop better control of crystallization, the experimental challenges to probing the transient events that control nucleation are formidable. Thus, there have been few experimental investigations, and, consequently, theory and modeling have been restricted to using empirical parameters to fit data. Clearly, there is a need for in situ investigations of crystallization that provide insight into flow-induced pathways to nucleation and subsequent morphological development and into the influence of molecular characteristics (such as molecular mass distribution and chain architecture) on these pathways.

While nucleation in quiescent crystallization[3] is predominantly heterogeneous, the dramatic increase in the number of nuclei per unit volume induced by flow appears to originate from the melt itself,[4] viz., homogeneously. Homogeneous nucleation has traditionally been viewed in terms of classical nucleation theory, which assumes that critical nuclei are formed through addition of units to compact clusters of the new phase. The formation of homogeneous primary nuclei in polymers (which develop far from equilibrium and are probably not compact) is not expected to be adequately described by classical nucleation theory (CNT). Nevertheless, as in CNT, the rate of nucleation is governed by the interplay between the driving force for crystallization and the mobility of the polymer chains. Thus, the nucleation rate, r^*, is expected to go to zero near the glass transition temperature of the polymer, T_g (where the polymer chain mobility goes to zero) and near the equilibium melting point, T_{Mo} (where the driving force for crystallization vanishes) and is expected to go through a maximum in between. These trends for r^* are experimentally observed in quiescent crystallization experiments on a variety of polymers.[3] In the context of the data presented here, it is significant to note that

---

* To whom correspondence should be addressed. E-mail: jak@cheme.caltech.edu. Fax: (626) 568-8743.

[†] Present address: Division of Polymer Chemistry, National Chemical Laboratory, Pune 411008, India.

[‡] California Institute of Technology.

[§] State University of New York, Stony Brook.

10.1021/ma0114180 CCC: $22.00

in the quiescent crystallization studies reported in the literature, the nucleation rate far above T_g is observed to decrease exponentially as the crystallization temperature approaches the melting point.

Recent studies indicate that the formation of critical nuclei in a variety of nonpolymeric systems[5,6] may be mediated by metastable intermediates; viz., nucleation may proceed along pathways not described by classical nucleation theory. These studies have prompted investigations of "nonclassical" pathways to nucleation in polymers as well. For example, researchers have suggested that homogeneous primary nucleation in polymer crystallization might be preceded by a spinodal liquid−liquid phase separation[7] or by the formation of stable protocrystalline aggregates.[8,9]

The influence of flow on polymer crystallization remains even more mysterious than the pathways to quiescent crystallization. Phenomenologically, it is well-known that upon imposition of flow, the crystallization kinetics are accelerated,[3] nucleation density is increased[10,4] and oriented crystalline morphologies often develop.[3,11,12] Keller and co-workers[13] have speculated that a coil−stretch transition mediated by strong flows precedes the formation of oriented crystals during flow-induced crystallization, while McHugh and co-workers[14] have suggested that oriented crystallization from flowing solutions might be preceded by an amorphous−amorphous phase separation. Others have reported the formation of ordered intermediate phases prior to crystallization during extrusion of polyethyelene[15] and during strain-induced crystallization of polar polymers such as poly(ethylene terephthalate) and its copolymers.[16]

Thus, there is considerable debate in the literature as to the route followed by polymers as they crystallize. As the crystallization behavior (e.g., lamellar thickness, crystallization half-time, final level of crystallinity) might be determined by the intermediate states that lead to nucleation, it is important to characterize the pathway to crystallization by in situ real time studies. Here, we focus on the activation barrier to nucleation, specifically how it is altered when flow perturbs the orientation distribution of the molecules. We present evidence that flow-induced nucleation during shear-enhanced crystallization is indeed mediated by a kinetic pathway.

2. Experimental Section

Novel instrumentation developed in our laboratory[17−19] is used to implement the "short-term" shearing protocol (Figure 1a) developed by Liedauer et al.[20,21] With our instrument, processing-like, intense shear stress[18] can be accessed, and sample requirements are small (500 mg/experiment). The experimental protocol (Figure 1a) imposes a well-defined thermal and flow history, allows us to isolate the effect of flow on crystallization from extraneous thermal effects and minimizes flow-induced reorientation of already formed crystallites. Initially, the polymer is held at 225 °C, above its equilibrium melting temperature ($T_{\mathrm{Mo}} \approx 208$ °C), to erase its flow history and to completely melt residual crystallites. Then, it is cooled to the desired crystallization temperature, T_{cryst} and held isothermal. The polymer is then sheared at a constant wall shear stress (σ_w) for a brief interval (short compared to the time for crystallization) using pressure-driven channel flow through a slit (6.3 cm long × 0.635 cm wide × 0.05 cm thick). Due to the high aspect ratio of the slit cross-section, the flow is quasi two-dimensional in the central region examined. While the applied wall shear stress and duration of shear are known, the transient velocity profile and total accumulated wall shear strain can only be estimated, as discussed in the Supporting Information (see paragraph at end of paper).

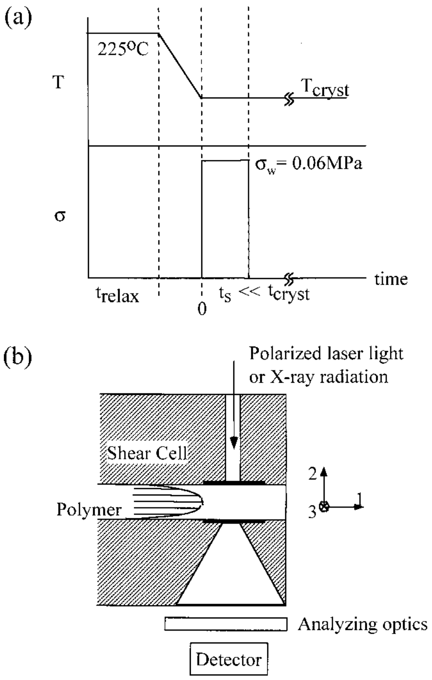

Figure 1. (a) Schematic representation of the "short-term shearing" experimental protocol[20]. Polarimetry and WAXD measurements are made *during* flow, (viz. during t_s) and after shear cessation (viz. during t_{cryst}). (b) Schematic of the shear cell constructed to implement the experimental protocol. The flow (1), velocity gradient (2), and vorticity (3) axes are as indicated.

Here, we report experiments using a combination of techniques to observe structure development in situ. We use polarimetry to resolve dynamics on millisecond time scales and synchrotron wide-angle X-ray diffraction (WAXD) to track structural evolution on time scales of a few seconds (Figure 1b). In the polarimetry experiments, red HeNe laser light (λ = 633 nm) polarized at 45° to the flow direction was incident on the sample. After passing through the sample, the light was analyzed using a polarizing beam splitter aligned at −45° to the flow. The intensity between crossed polars can be related to the birefingence in the velocity-vorticity plane, Δn_{13}, averaged over the velocity gradient direction. The birefringence is a measure of anisotropy in the flow-vorticity plane and arises from melt orientation, as well as crystallites or other ordered structures oriented in the flow direction. Synchrotron WAXD was carried out at beamline X27C of the National Synchrotron Light Source, Brookhaven National Laboratory, using an X-ray wavelength of 1.307 Å. Here too, the radiation was incident along the velocity-gradient direction, normal to the flow-vorticity plane. Details of the experimental setup for the rheo-birefringence measurements[17] and the rheo-WAXD[19] measurements have been previously described.

In the first part of the paper, we report experiments using a polydisperse Ziegler−Natta isotactic polypropylene, PP-300/6 ($M_w \approx$ 300 000 g/mol, PDI ≈ 6−8, isotactic pentad content [mmmm] ≈ 96%, melt flow index = 12 dg/min at 230 °C/2.16 kg load). This is then contrasted with the behavior of model polymers: two iPP samples with matched stereoregularity, but very different mean chain lengths: "long" chains ($M_w \approx$ 825 000 g/mol, $M_w/M_n \approx 2.8$) and "short" chains ($M_w \approx$ 180 000 g/mol, $M_w/M_n \approx 2.1$) and a bidisperse blend containing 2% of the "long" chains mixed with 98% of "short" chains. The isotactic pentad content of "short" is [mmmm] = 95.4% as determined by solution NMR. The "long" and "short" polymers have well matched quiescent crystallization and melting behavior as observed by differential scanning calorimetry, and similar stereoregularity as evident from their IR spectra (ratio of bands at 998 and 973 cm^{-1}).

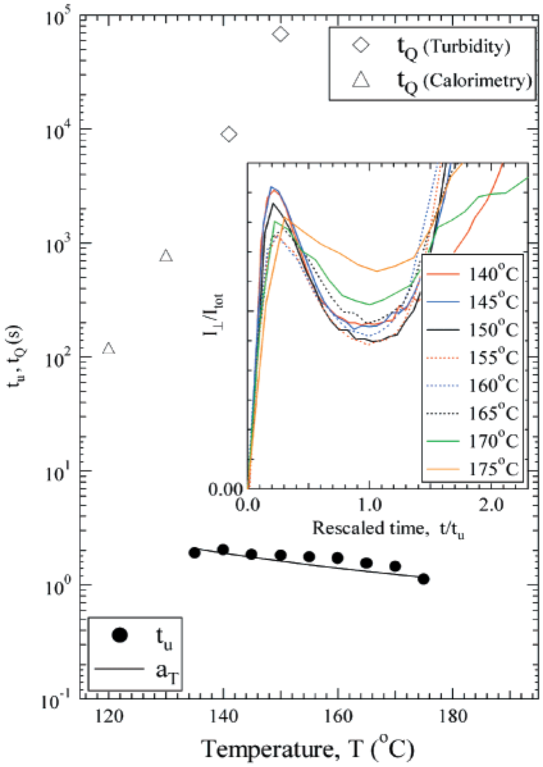

Figure 2. Temperature dependence of the time scale for quiescent crystallization, t_Q, and of the time to inception of the unusual upturn in birefringence during shear, t_u. The triangles are peak times for crystallization measured using differential scanning calorimetry while the diamonds are the time to reach turbidity of 0.5 during quiescent crystallization experiments in our flow device. t_u was obtained as the lowest point of a parabola fitted to the birefringence trace near the upturn (inset shows birefringence traces plotted against rescaled time, t/t_u). The solid line is the WLF rheological shift factor[35] with respect to a reference temperature of 190 °C.

The model bidisperse samples were prepared by solution blending (3% solution by weight in xylene at 120 °C for 20 min with a few thousand ppm of antioxidant, Irganox 1010, Ciba Chemicals, added to prevent degradation) and then precipitated by adding slowly into a large (8-fold) excess of cold, continually stirred methanol. The precipitate was then extensively washed with methanol and vacuum-dried at 70 °C for at least 2 days. To evaluate the effects of the solution blending experimental protocol on the polymer, control experiments were done where pure “short” iPP was subjected to the same procedure used to prepare the blends. Rheological measurements (oscillatory dynamical mechanical measurements at low frequencies) indicated very little, if any, degradation for the dissolved, precipitated and dried polymer as compared to the virgin resin. The treated iPP crystallized more rapidly than the virgin material, but similar to the case of the virgin material, oriented crystallites were not observed in our shear experiments.

3. Results

In all the experiments described in this paper, we employ a wall shear stress, $\sigma_w = 0.06$ MPa, previously established[17,19] to be large enough to induce a transition to oriented crystallite growth in PP-300/6 at a crystallization temperature of $T_{cryst} = 141$ °C. We report results of our investigations on the effect of T_{cryst} on the time of formation of oriented crystals. Even at the deepest subcooling investigated (viz., lowest T_{cryst}, 141 °C), the quiescent crystallization time, t_Q, for this polymer is on the order of hours (Figure 2), significantly longer than the shearing durations employed ($t_s \leq 12$ s). Upon cessation of flow, polymer chains in the melt rapidly relax[17,22] to a quiescent, isotropic state.

Upon application of a high stress, the polymer chains undergo nonlinear stretching,[23] manifested as an overshoot in the birefringence[17,24] (Figure 2, inset). Since fixed σ_w gives rise to approximately the same average orientation of polymer chain segments in the melt,[1] the magnitude of the birefringent overshoot does not vary much over the range of T_{cryst}. Unlike an amorphous polymer melt, the birefringence does not attain a steady state after the overshoot; instead the birefringence shows an unusual upturn and continues to increase monotonically, indicating the formation of a long-lived oriented structure.[17,25] Furthermore, we note that the time at which the birefringent upturn begins, t_u, *decreases* with increasing temperature up to the highest investigated $T_{cryst} = 175$ °C (above the nominal melting point, $T^m{}_{nom} \approx 170$ °C, determined as the point at which the crystallites are observed to melt upon heating, but substantially below the equilibrium melting temperature, $T_{Mo} \approx 208$ °C). Interestingly, the behavior of t_u tracks the temperature dependence of polymer chain dynamics in the melt as it follows the rheological Williams–Landel–Ferry (WLF) time–temperature shift factor (Figure 2). We could not establish the upper limit in temperature for the creation of oriented precursors due to the limited sample (from the same lot) that was available.

In situ synchrotron WAXD confirms that at 141 and 163 °C crystalline peaks corresponding to the α-monoclinic phase of iPP[26] appear during shear on the same time scale as the birefringent upturn—in a matter of a few seconds (Figure 3a,b), which is orders of magnitude faster than the quiescent crystallization time (Figure 2). Two-dimensional WAXD patterns obtained as the polymer is sheared show that flow induces highly oriented crystallites with their chain (c) axis along the flow direction[27] (Figure 4). Thus, as shown earlier,[17,19] the appearance of the upturn in the birefringence signal correlates with the formation of flow-oriented crystallites. Above 163 °C, it was not possible to use WAXD to directly confirm this correlation since crystalline peaks cannot be resolved from the noise during shear (Figure 3c,d). Nevertheless, the development of highly oriented crystallinity after cessation of flow (Figure 3c, and two-dimensional WAXD not shown) on time scales orders of magnitude faster than quiescent crystallization (extrapolated to be $t_Q \approx O(10^6$ s) based on quiescent data shown in Figure 2) suggests that the birefringent structures generated during shear are responsible for the formation of the crystallites. However, for temperatures above the nominal melting point, $T^m{}_{nom}$, crystalline peaks are never observed (Figure 3d).

The unusual temperature dependence of the time for development of the oriented precursors (Figure 2), suggests that their formation during flow might be rheologically controlled. The upturn in the birefringence at different T_{cryst} occurs at approximately the same value of time rescaled by the rheological shift factor. If the behavior of the flowing material is largely meltlike until $t \simeq t_u$, then our data indicate that the appearance of the birefringent upturn happens at a fixed strain (see Supporting Information). Thus, the controlling time scale for induction of oriented precursors is determined either by the time to reach a given macroscopic strain or by the time for the polymer molecules to reach a critical level of molecular orientation. To differentiate

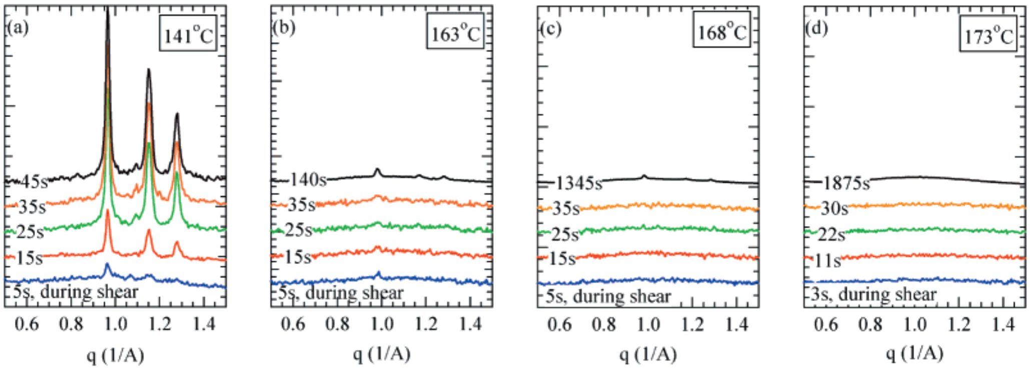

Figure 3. Evolution of WAXD intensity during and after cessation of shear at (a) 141, (b) 163, (c) 168, and (d) 173 °C. The one-dimensional traces presented were obtained by taking a slice of the two-dimensional WAXD pattern perpendicular to the flow direction (see Figure 4) and have been normalized for acquisition time at each temperature.

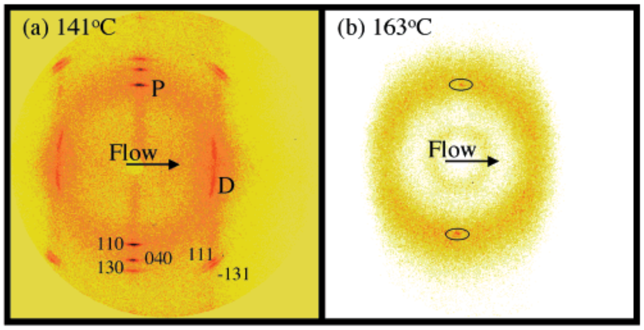

Figure 4. Two-dimensional oriented WAXD patterns obtained during shear at (a) 141 and (b) 163 °C. The diffracting planes are as indicated. "Parent" crystallites (P) are observed with the polymer chain (*c*) axis along the flow direction. As expected, at the lower crystallization temperature (a), these are accompanied by epitaxial "daughter" (D) crystallites oriented at approximately ±80° with respect to the parents. At higher temperatures (b), faint 110 peaks from the *c* axis oriented crystals can be seen in the indicated areas.

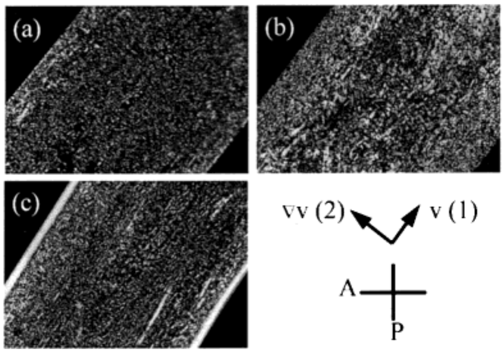

Figure 5. Ex situ polarized light micrographs of isotactic polypropylenes subjected to short-term shearing, viewed through crossed polarizers (oriented as indicated). Polymer in a 500 μm slit is driven by a pressure drop along the velocity direction (v, axis 1 in Figure 1b) for a time t_s under isothermal conditions (T_{cryst} = 142 °C). During t_s the shear stress is a maximum at the walls ($\sigma_w \approx$ 0.1 MPa), decreasing linearly to zero at the center of the sample. Samples "short" and "long" are described in the text. (a) "Short" iPP sheared for t_s = 2.2 s (wall shear strain, $\gamma_{ge} \approx$ 100). (b) "Long" iPP sheared for t_s = 300 s. (c) A blend of 2% long and 98% short sheared for t_s = 2.25 s. The introduction of a controlled high molecular weight tail enables the shear-induced formation of oriented precursors manifested by the highly oriented skin (bright when viewed through crossed polars).

between these scenarios, we examine the shear-induced crystallization of "long" and "short" chains, such that the long chains have a relaxation time over 2 orders of magnitude greater than the short chains ($\tau_L/\tau_S \approx 160$). These model materials were crystallized after shearing at a high wall shear stress, σ_w = 0.1 MPa. Their behavior is compared at fixed applied stress (rather than at the same shear rate) so that the average orientation induced by flow is similar in each case. The "short" chain melt was sheared for t_s = 2 s, which corresponded to the strain limit of our instrument, $\gamma_{ge} \approx 100$, while the high viscosity "long" chain melt was sheared for t_s = 300 s. The narrow distribution materials were allowed to crystallize for several hours during which time they became completely opaque (no transmitted light could be observed with our detectors), and were then extracted from the shear apparatus and rapidly transferred to a cold water bath. Images in the flow-velocity gradient plane, viewed between crossed polarizers, show that these polymers do not form oriented crystallites even after being subjected to such intense shearing (Figure 5a,b). However, when a blend containing a small amount (2, 5, or 10%) of the "long" chains homogeneously dispersed a matrix of "short" chains, is sheared at the same wall shear stress for t_s = 2.25 s ($\gamma_{ge} \approx 100$), oriented crystallites are readily induced (Figure 5c). We note here that the addition of 2% "long" chains to the "short" matrix hardly perturbs its rheological properties, so that both the total strain ($\gamma_{ge} \approx 100$) and the shearing time (t_s = 2.25 s) for the blend were very similar to the conditions used for the pure "short" material. These results indicate a mechanism for flow-enhanced crystallization based on molecular orientation, rather than a mechanism based on achieving a given level of strain. We explore this idea in greater depth in the Discussion.

4. Discussion

In this paper, we focus on two central aspects of the effect of flow on crystallization: first, our results indicate that flow opens a kinetic pathway to nucleation in isotactic polypropylene; furthermore, observations on the bidisperse blends of model narrow distribution resins indicate that this pathway is mediated by molecular orientation, particularly that of the chains that are most highly distorted during flow.

The combination of in situ birefringence and WAXD with ex situ microscopy (presented previously[17,19]) clearly shows that the upturn in the birefringence signal observed during shear correlates with the subsequent formation of oriented crystals at T_{cryst} = 141 °C. Here, we observe that the birefringent signature can be observed at temperatures up to 175 °C (inset, Figure

2). While these temperatures are substantially below the equilibrium melting temperature of α-iPP, $T_{\mathrm{Mo}} \approx$ 208 °C, they are close to the temperature at which crystal growth velocities approach zero, called the nominal melting temperature, $T^{\mathrm{m}}_{\mathrm{nom}} \approx 170$ °C. Slightly below $T^{\mathrm{m}}_{\mathrm{nom}}$ (at $T_{\mathrm{cryst}} = 168$ °C), highly oriented crystallites appear after flow cessation (Figure 3, and 2-dimensional WAXD, not shown), indicating that oriented precursors did form during flow, but crystallites growing from these precursors can be detected by WAXD only at later times. However, synchrotron-WAXD acquired rapidly *during shear* detects crystalline peaks (corresponding to the α form[26]) only up to 163 °C (Figure 4). Comparison of the birefringence and WAXD data leads us to infer that the oriented structures that develop during flow are *flow-induced crystallization precursors*. At temperatures below $T^{\mathrm{m}}_{\mathrm{nom}}$, α-iPP crystallites grow off these precursors and persist even after flow cessation. These oriented crystallites amplify the birefringence and explain its persistence. Above $T^{\mathrm{m}}_{\mathrm{nom}}$, α-crystallites do not grow off the birefringent precursors formed during shear; after cessation of shear, the birefringence relaxes completely, and no development of crystallinity is observed by WAXD.[28]

In the experiments described here, the sample is subjected to a controlled stress, and the same stress is used across the series of experiments at different temperatures. This holds the overall level of molecular orientation nearly fixed, exposing the role of temperature. It is interesting to note that the relative time scales at which a comparable level of crystallinity begins to develop in the WAXD data ($\sim O$ (1 s) at 141 °C, $\sim O$ (100 s) at 163 °C at $\sim O$ (1000 s) for 168 °C, Figure 3) are inversely proportional to the relative linear crystal growth rates (extrapolated from the literature:[29,30] $\sim O$ (10^{-7} cm/s) at 141 °C, $\sim O$ (10^{-9} cm/s) at 163 °C and $\sim O$ (10^{-10} cm/s) at 168 °C). Since the relaxation time for the polymer melt after flow cessation is very short[22] at the experimental T_{cryst} ($\gg T_{\mathrm{g}}$), and since the linear crystal growth rate is unchanged for different nucleation geometries,[31] it is reasonable to assume that the crystals growing from the precursors grow in a stress-relaxed melt, at their quiescent growth velocities. Thus, the relative time scales at which WAXD crystallinity is evident with increasing temperature suggest that nucleation occurs during the brief flow interval and that crystals grow from these flow-induced nuclei to form the oriented crystallites observed in the WAXD at later times. Furthermore, the quantitative correlation between the time to reach comparable crystallinity and the relative growth velocities suggest that the length of “threadlike precursors” per unit volume is similar in all three cases.

The observation of oriented nucleation precursors at temperatures above $T^{\mathrm{m}}_{\mathrm{nom}}$ (Figure 2d) is consistent with prior studies[32,33,34] that demonstrated that an iPP melt retained memory of shearing at temperatures greater than $T^{\mathrm{m}}_{\mathrm{nom}}$, rapidly forming oriented α-crystallites on cooling below $T^{\mathrm{m}}_{\mathrm{nom}}$ after flow cessation. Thus, the birefringent upturn that we observe in our experiments represents a signature of the oriented precursors to crystallization, even at $T > T^{\mathrm{m}}_{\mathrm{nom}}$.

The most surprising aspect of our data is that the time for these precursors to appear, t_{u}, *decreases* with increasing temperature, in stark contrast to the exponential increase observed for the quiescent crystallization time, $t_{\mathrm{Q}}(T)$, attributed largely to the activation barrier for creating a critical nucleus (Figure 2). The main signature of the activation barrier to formation of a critical nucleus—the slowing of crystallization as the subcooling decreases—is eliminated. Furthermore, the temperature dependence of t_{u} is strikingly similar to that of the dynamics of polymer chains in the melt, described by the rheological time–temperature shift factor, a_{T}[1,35] (solid curve, Figure 2). Thus, the formation of the precursors to nucleation tracks the dynamics of the polymer molecules in the melt. This rheologically controlled pathway to nucleation is unanticipated by existing models,[20,36–38] which retain the temperature dependence observed in quiescent crystallization, and, consequently, cannot predict a decrease in the time for inception of crystallization with increase in temperature. Under intense shear, nucleation appears to proceed via a kinetic pathway that effectively eliminates the activation barrier for nucleation.

Our experiments examining the role of molecular mass distribution show that while intense shear does *not* induce the formation of oriented crystals in narrow molecular weight resins, introducing a distribution of relaxation times in the melt by addition of a small percentage of high molecular weight chains to a low molecular weight resin gives shear-induced oriented morphologies. The role of the “long” chains suggests a molecular mechanism for flow-mediated anisotropic nucleation.[39] A fixed σ_{w} generates approximately the same average level of orientation of chain segments. In a material with a fairly narrow distribution of molecular weights, all chains explore similar anisotropic configurations. On the other hand, in a material that contains a small fraction of chains that are much longer than average and that overlap,[39] the slow relaxing (long) molecules are much more strongly perturbed from their equilibrium configuration than the average anisotropy induced by the given stress,[40] and form an anisotropic “scaffolding”. Distorted chain conformations increase the local concentration of chain segments that are roughly parallel to one another. In turn, this may increase the probability that these segments explore a stable, long-lived configuration due to thermal motion. The oriented local configurations generated in the vicinity of the highly distorted, slowly relaxing species appear to preferentially form the precursors for oriented nucleation and determine the threshold stress. It appears that, at high shear stress, the rate of formation of these stable precursors by this orientation-enhanced pathway is so great that the usual activation barrier is no longer relevant to the formation of crystallization precursors. The rate-limiting process for precursor formation appears to be the time to generate a sufficiently distorted chain conformation.

In establishing the role of long chains, the availability of model materials is essential. We use relatively narrow distribution ($M_{\mathrm{w}}/M_{\mathrm{n}} \approx 2-3$) samples of isotactic polypropylene that have uniform and matched stereo- and regiodefect content. Therefore, the effect of the long chains in the bidisperse blend cannot be attributed to higher stereo regularity (in contrast to typical Ziegler–Natta iPPs in which the longest chains are also the most stereoregular[41]), clearly exposing the effect of chain length itself. Our experiments provide the first unambiguous demonstration of the role played by chain length distribution in the shear-induced formation of oriented crystals, building on the pioneering work of

Keller[42] and Janeschitz-Kriegl[43] who were confronted with complex, poorly defined materials.

The kinetic pathway that opens up in our system under the influence of a strong applied field might have general relevance to the current debate regarding the importance of metastable pathways in mediating phase transitions. Researchers have observed that the crystallization of polymers and low molecular weight materials can be mediated by ordered intermediate phases. For example, the metastable rotator phase in short chain *n*-alkanes[5] and its thermodynamically continuous counterpart in polyethylene,[44] the hexagonal phase (observed for crystallization at high pressures[44] or during extrusion[15]), have been implicated in mediating the formation of the stable crystal phase. For rigid, polar polymers such as PET or PET/PEN copolymers, Mahendrasingam and co-workers[16] have inferred the formation of an oriented smectic mesophase prior to crystallization during straining. They concluded that the strain-influenced formation of the oriented, ordered mesophase mediated the process of crystallization and led to the observed acceleration in the kinetics of phase transformation. The precursors observed in our flow experiments appear to be very different from such ordered crystallization precursors. The WAXD peaks that we observe come from the stable monoclinic phase of iPP, even at the earliest time for which crystallinity can be detected; rotator-type or analogous phases have never been observed during crystallization of iPP. Our experiments with the bidisperse blends clearly identify the rheological origin of the flow-induced precursors, while the ordered precursors discussed above are not expected to be strongly dependent on molecular weight distribution. Furthermore, in the experiments with the polar polymers,[16] the smectic mesophase is formed during straining near the glass transition temperature. Therefore, the intermediate phase might arise from the creation of hydrogen-bonding stabilized ordered domains formed due to strain-induced chain disentanglement. Such a mechanism has been previously observed to accelerate crystallization in nylons[45] where it was called a “melt−memory effect”.

Other researchers have suggested that the appearance of scattered intensity at small angles prior to the appearance of crystalline reflections at wide angles during simultaneous small and wide-angle X-ray scattering measurements of crystallizing polymers is indicative of an intermediate state in the melt-solid transition.[46] Olmstead et al.[7] have accounted for the unexpected time dependence of the scattering data by suggesting that the polymer melt undergoes a spinodal liquid−liquid-phase transition when cooled from above the equilibrium melting point, and that primary nucleation occurs from the metastable “dense” liquid phase. We have performed small and wide angle synchrotron X-ray scattering[47] to monitor the evolution of crystalline structure during and after shearing. Within the time resolution and sensitivity of our experiments, SAXS and WAXD appear together. Thus, we have no evidence for crystallization being preceded by the separation of the melt into more and less dense regions. WAXD is not sensitive enough to unambiguously identify the structure of the oriented birefringent-precursor induced by flow in our experiments. However, due to their effectiveness in mediating the nucleation of oriented α-iPP crystallites, we speculate that these precursors present an epitaxial match to α-iPP with chain axis along the flow direction.

McHugh[14] has observed amorphous precursors in seeded-growth crystallization experiments on flowing polymer solutions and has suggested that a liquid−liquid phase separation precedes the formation of oriented crystals. However, in work published previously by our group,[17] we observe no evidence for an amorphous phase separation in flow-crystallization experiments.

Janeschitz-Kriegl and co-workers[8,9] have invoked a size-dependent surface tension for the nucleus−melt interface[48] to postulate the formation of stable protocrystalline aggregates (athermal nuclei) below a “limiting temperature for metastability” (estimated to be about 170 °C for iPP). They speculate that these athermal nuclei coalesce due to flow-induced collisions during shear, leading to enhancement in nucleation and effective crystallization rates.[49] Our observation that the shear-induced structure leads to oriented crystallite growth below 170 °C accords well with the “metastability limit” estimated by Janeschitz-Kriegl and co-workers. However, the temperature dependence of the formation of the birefringent precursors does not indicate that nucleation is a result of the coalescence of “athermal nuclei”. With an increase in temperature from 140 to 170 °C, Janeschitz-Kriegl and co-workers[9] estimate that the number of athermal nuclei is reduced by about 3 orders of magnitude. The formation of precursors in our experiments, however, happens during flow at about the same time scale even as the temperature is increased through this range. Thus, while there are certain aspects of the framework laid out by Janeschitz-Kriegl and co-workers that accord well with our data, we do not believe that the kinetic nucleation pathway observed in these experiments is due to enhanced convective coagulation of athermal nuclei.

Keller and co-workers[13] conducted elongational flow experiments with polyethylene solutions and observed that the oriented crystals that were formed under intense flow conditions were preceded by strong birefringence observed in the flow apparatus. They speculated that polymer chains above a “critical orientation molecular weight”, M^*, underwent a coil−stretch transition when subjected to elongational flow prior to crystallization and that the stretching transition was a prerequisite for the formation of oriented crystals. However, no method to determine M^* was proposed. While a coil−stretch transition has been inferred for dilute solutions of polymers in extensional flow,[13] there is no direct evidence for such a transition in an entangled melt undergoing shear flow. We found no evidence for a coil−stretch transition in experiments where an atactic polypropylene was subjected to intense shearing in our flow apparatus.[17] Nevertheless, Keller’s insight that the longest chains become much more oriented than average appears to play a central role.

Recently, Somani et al.[50] have proposed a method to infer M^* from small-angle X-ray scattering measurements during shear-induced oriented crystallization of a highly polydisperse iPP. Their analysis assumes that the fraction of row-nucleated crystallites bears a one-to-one correspondence with the portion of chains in the sample that undergo significant extension, viz. chains with a molecular weight exceeding M^*. However, our results indicate that the addition of just 2% of “long” chains that have a molecular weight approximately fivetimes that of the "short" chains can cause the formation of oriented crystallites that greatly exceed 2% of all the crystallites (in the oriented skin, virtually all of the crystallites are oriented). Indeed, the long chain content in these well-defined materials is so low that it would be difficult to quantify by GPC or rheology. The row-nucleated morphology explains how a small concentration of long chains can cause a large fraction of oriented growth: the addition of long chains leads to the formation of threadlike precursors, which nucleate highly oriented growth due to the lateral constraint of lamellae simultaneously growing radially outward from a central thread. The oriented lamellae that grow involve all the chains present in the melt, greatly amplifying the oriented growth represented by the threadlike precursors themselves. Thus, there is still no means to determine M^* within a given broad distribution material. Model bidisperse blends of well-defined iPP open the way to determine the interplay of chain length, stereoregularity and concentration of long chains that governs the flow-induced formation of oriented precursors to crystallization.

5. Conclusions

In situ rheo-optical techniques combined with synchrotron wide-angle X-ray scattering (WAXD) reveal the emergence and structure of oriented crystallization precursors that develop upon strongly shearing an isothermal melt of polydisperse isotactic polypropylene (iPP). The time for these precursors to appear *decreases* with increasing temperature, tracking the melt dynamics of the polymer molecules. This surprising result suggests that, under intense shear, the nucleation of oriented crystallites is governed by the rheologically determined formation of a critical anisotropic configuration of polymer chains in the melt. Model bidisperse systems containing a small percentage of high molecular weight iPP blended with lower molecular weight iPP of matched stereoregularity demonstrate that this "nonclassical" pathway to nucleation is mediated by chains that access above-average orientation during flow. Beyond implications for polymer processing, similar pathways may be important in other systems as well.

Acknowledgment. We are grateful to Dr. A. Prasad (Equistar Chemical) for providing us with the polydisperse polymer used in this study and to Dr. R. L. Sammler (The Dow Chemical Co.) for providing us with the narrow distribution polymers. We thank Dr. Motohiro Seki (Mitsubishi Chemical Co.) for NMR tacticity determination and Dr. Markus Gahleitner (Borealis AG) for measuring the Chisso IR tacticity. Synchrotron experiments were carried out at the beamline X27C of the National Synchrotron Light Source, Brookhaven National Laboratory, which is supported by the US Department of Energy, Divisions of Material Sciences and Chemical Sciences under Contract Number DE-AC02-98CH10886. We are grateful to Dr. Weidong Liu, P. Wang, and Y. Sun for assistance with synchrotron measurements and to Prof. R. C. Flagan (Caltech) for helpful discussions and for critiquing this manuscript. Financial support from Procter and Gamble, the Cargill-NIST ATP, the Schlinger Fund, and the NSF (DMR9901403) is gratefully acknowledged.

Supporting Information Available: Text explaining the challenges encountered in estimating the wall shear strain in a material whose structure is changing with time during flow and a figure illustrating a method to determine if the effective viscosity is increased due to structure development. This material is available free of charge via the Internet at http://pubs.acs.org.

References and Notes

(1) Doi, M.; Edwards, S. F. *The Theory of Polymer Dynamics*; Oxford Publications: Oxford: 1986.
(2) Meijer, H., Ed.; *Processing of Polymers*; volume 18 VCH (NY): 1997.
(3) van Krevelen, D. *Chimia* **1978**, *32*, 279–294.
(4) Wolkowicz, M. D. *J. Polym. Sci.* (*Polym. Symp.*) **1978**, *63*, 365–382.
(5) Sirota, E. B.; Herhold, A. B. *Science* **1999**, *283*, 529–532.
(6) tenWolde, P. R.; Frenkel, D. *Science* **1997**, *277*, 1975–1978. Talanquer, V.; Oxtoby, D. W. *J. Chem. Phys.* **1998**, *109*, 223–227. Yau, S.-T.; Velikov, P. G. *Nature* **2000**, *406*, 494–497. tenWolde, P. R.; Oxtoby, D. W.; Frenkel, D. *Phys. Rev. Lett.* **1998**, *81*, 3695–3698. McClurg, R. B.; Flagan, R. C.; Goddard, W. A. *Nanostruct. Mater.* **1997**, *9*, 53–61.
(7) Olmstead, P.; Poon, W.; McLeish, T.; Terrill, N.; Ryan, A. *Phys. Rev. Lett.* **1998**, *81*, 373–376.
(8) Janeschitz-Kriegl, H. *Colloid Polym. Sci.* **1997**, *275*, 1121–1135.
(9) Janeschitz-Kriegl, H.; Ratajski, E.; Wippel, H. *Colloid Polym. Sci.* **1999**, *277*, 217–226.
(10) Haas, T.; Maxwell, B. *Polym. Eng. Sci.* **1969**, *9*, 225–241.
(11) Binsbergen, F. L. *Nature* **1966**, *211*, 516–517.
(12) Keller, A.; Machin, M. J. *J. Macromol. Sci.* (*B*) **1967**, *1*, 41–91.
(13) Keller, A.; Kolnaar, H. W. H. Flow Induced Orientation and Structure Formation. In *Processing of Polymers*; Meijer, H. E. H., Ed.; VCH: Weinheim, Germany, 1997, Vol. 18.
(14) Rietveld, J.; McHugh, A. J. *J. Polym. Sci.* (*Polym. Lett.*) **1983**, *21*, 919–926. McHugh, A. J.; Blunk, R. H. *Macromolecules* **1986**, *19*, 1249–1255. McHugh, A. J.; Spevacek, A. J. *J. Polym. Sci.* (*Polym. Phys.*) **1991**, *29*, 969–979.
(15) Kolnaar, J. W. H.; Keller, A.; Seifert, S.; Zschunke, C.; Zachmann, H. G. *Polymer* **1995**, *36*, 3969–3974.
(16) Mahendrasingam, A.; Martin, C.; Fuller, W.; Blundell, D. J.; Oldman, R. J.; Harvie, J. L.; MacKerron, D. H.; Riekel, C.; Engstroem, P. *Polymer* **1999**, *40*, 5533–5565. Mahendrasingam, A.; Martin, C.; Fuller, W.; Blundell, D. J.; Oldman, R. J.; MacKerron, D. H.; Harvie, J. L.; Riekel, C. *Polymer* **2000**, *41*, 1217–1221. Blundell, D. J.; Mahendrasingam, A.; Martin, C.; Fuller, W. *J. Mater. Sci.* **2000**, *35*, 5057–5063. Welsh, G. E.; Blundell, D. J.; Windle, A. H. *J. Mater. Sci.* **2000**, *35*, 5225–5240.
(17) Kumaraswamy, G.; Issaian, A. M.; Kornfield, J. A. *Macromolecules* **1999**, *32*, 7537–7547.
(18) Kumaraswamy, G.; Verma, R. K.; Kornfield, J. A. *Rev. Sci. Instrum.* **1999**, *70*, 2097–2104.
(19) Kumaraswamy, G.; Verma, R. K.; Issaian, A. M.; Wang, P.; Kornfield, J. A.; Yeh, F.; Hsiao, B. S.; Olley, R. H. *Polymer* **2000**, *41*, 8931–8940.
(20) Liedauer, S.; Eder, G.; Janeschitz-Kriegl, H.; Jerschow, P.; Geymayer, W.; Ingolic, E. *Int. Polym. Process.* **1993**, *8*, 236–244.
(21) Liedauer, S.; Eder, G.; Janeschitz-Kriegl, H. *Intern. Polym. Process.* **1995**, *10*, 243–250.
(22) Linear viscoelastic measurements on the iPP melt at 190 °C indicate a stress relaxation time scale of $\sim O$ (ms). Indeed, after cessation of shear, the flow birefringence decreases rapidly, on a time scale of a few tens of milliseconds even at the lowest T_{cryst}[17] for the experiments reported here.
(23) Menezes, E. V.; Graessley, W. W. *J. Polym. Sci.* (*Polym. Phys.*) **1982**, *20*, 1817–1833.
(24) Janeschitz-Kriegl, H. *Polymer Melt Rheology and Flow Birefringence*; Springer-Verlag: Berlin, 1983.
(25) After cessation of shear, the melt birefringence decreases rapidly to a nonzero residual value.[17] The initial drop in the melt birefringence can be attributed to stress-relaxation processes in the melt, while the residual value suggests that the imposition of stress has led to the formation of "long-lived" oriented structures, that persist even after cessation of flow.
(26) Jones, A. T.; Aizlewood, J. M.; Beckett, D. R. *Makromol. Chem.* **1964**, *75*, 134–158.
(27) Padden, F. J., Jr.; Keith, H. D. *J. Appl. Phys.* **1966**, *37*, 4013–4020. Binsbergen, F. L.; Lange, B. G. M. D. *Polymer* (*London*) **1968**, *9*, 23–40. Lotz, B.; Wittmann, J. C.; Lovinger, A. J. *Polymer* **1996**, *37*, 4979–4992.

(28) Wang et al. (Wang, Z. G.; et al. *Macromolecules* **2000**, *33*, 978−989) have shown that the detection limit for WAXD is about 1% crystallinity. This sets a lower bound for the observable crystallinity in our measurements.

(29) Janimak, J. J.; Cheng, S. Z. D.; Giusti, P. A.; Hsieh, E. T. *Macromolecules* **1991**, *24*, 2253−2260.

(30) Varga, J. Crystallization, Melting and Supermolecular Structure. In *Polypropylene*; Varga, J., Karger-Kocsis, J., Eds.; Chapman and Hill: New York, 1995; Vol. 1(Structure and Morphology), p 76.

(31) White, H. M.; Bassett, D. C. *Polymer* **1997**, *38*, 5515−5520.

(32) Alfonso, G. C.; Scardigli, P. *Macromol. Symp.* **1997**, *118*, 323−328.

(33) Eder, G.; Janeschitz-Kriegl, H. In *Processing of Polymers*; Meijer, H. E. H., Ed.; VCH: New York, 1997; Vol. 18.

(34) Eder, G.; Janeschitz-Kriegl, H.; Liedauer, S. *Prog. Polym. Sci.* **1990**, *15*, 629−714.

(35) Eckstein, A.; Suhm, J.; Friedrich, C.; Maier, R.-D.; Sassmannshausen, J.; Bochmann, M.; Mulhaupt, R. *Macromolecules* **1998**, *31*, 1335−1340.

(36) Ziabicki, A. *Colloid Polym. Sci.* **1974**, *252*, 207−221. Ziabicki, A. *Colloid Polym. Sci.* **1974**, *252*, 433−447.

(37) Bushman, A. C.; McHugh, A. *J. Polym. Sci.* (*Polym. Phys.*) **1996**, *34*, 2393−2407. Doufas, A. K.; Dairanieh, I. S.; McHugh, A. J. *J. Rheol.* **1999**, *43*, 85−109.

(38) Isayev, A. I.; Chan, T. W.; Shimojo, K.; Gmerek, M. *J. Appl. Polym. Sci.* **1995**, *55*, 807−819.

(39) Seki, M.; Thurman, D.; Oberhauser, J. and Kornfield, J. A. Shear-Mediated Crystallization of Isotactic Polypropylene: The Role of Long Chain-Long Chain Overlap. *Macromolecules*, in press.

(40) Brochard-Wyart, F.; DeGennes, P. G. *C. R. Acad. Sci. Paris* **1988**, *Ser. 2*, *306*, 699−702.

(41) Paukkeri, R.; Vaananen, T.; Lehtinen, A. *Polymer* **1993**, *34*, 2488−2494. Paukkeri, R.; Iiskola, E.; Lehtinen, A.; Salminen, H. *Polymer* **1994**, *35*, 2636−2643.

(42) Bashir, Z.; Odell, J. A.; Keller, A. *J. Mater. Sci.* **1984**, *19*, 3713−3725.

(43) Jerschow, P.; Janeschitz-Kriegl, H. *Int. Polym. Proc.* **1997**, *12*, 72−77.

(44) Ungar, G. *Macromolecules* **1986**, *19*, 1317−1324.

(45) Khanna, Y. P.; Reimschuessel, A. C.; Banerjie, A.; Altman, C. *Polym. Eng. Sci.* **1988**, *28*, 1600−1606. Khanna, Y. P.; Kumar, R.; Reimschuessel, A. C. *Polym. Eng. Sci.* **1988**, *28*, 1607−1611. Khanna, Y. P.; Kumar, R.; Reimschuessel, A. C. *Polym. Eng. Sci.* **1988**, *28*, 1612−1615.

(46) Imai, M.; Mori, K.; Mizukami, T.; Kaji, K.; Kanaya, T. *Polymer* **1992**, *33*, 4451−4456. Imai, M.; Mori, K.; Mizukami, T.; Kaji, K.; Kanaya, T. *Polymer* **1992**, *33*, 4457−4462. Imai, M.; Kaji, K.; Kanaya, T. *Macromolecules* **1994**, *27*, 7103−7108. Cakmak, M.; Teitge, A.; Zachmann, H. L.; White, J. L. *J. Polym. Sci.* (*Polym. Phys.*) **1993**, *31*, 371−381. Ezquerra, T. A.; Lopez-Cabarcos, E.; Hsiao, B.; Balta-Calleja, F. J. *Phys. Rev. E* **1996**, *54*, 989−992. Strobl, G., Ed.; *The Physics of Polymers*; Springer: Berlin, 1996. Ryan, A. J.; Fairclough, P. A.; Terrill, N. J.; Olmstead, P. D.; Poon, W. C. K. *Faraday Discuss., Chem. Soc.* **1999**, *112*, 13−29. Samon, J. M.; Schultz, J. M.; Hsiao, B. S.; Seifert, S.; Stribeck, N.; Gurke, I.; Collins, G.; Saw, C. *Macromolecules* **1999**, *32*, 8121−8132.

(47) Kumaraswamy, G. Ph.D. Thesis, California Institute of Technology, 2000.

(48) Tolman, R. C. *J. Chem. Phys.* **1949**, *17*, 333−337.

(49) Janeschitz-Kriegl, H. Personal communication.

(50) Somani, R. H.; Hsiao, B. S.; Nogales, A.; Srinivas, S.; Tsou, A. H.; Sics, I.; Balta-Calleja, F. J.; Ezquerra, T. A. *Macromolecules* **2000**, *33*, 9385−9394. Nogales, A.; Hsiao, B. S.; Somani, R. H.; Srinivas, S.; Tsou, A. H.; Balta-Calleja, F. J.; Ezquerra, T. A. *Polymer* **2001**, *42*, 5247−5256.

MA0114180